Flavone Synthases from *Medicago truncatula* Are Flavanone-2-Hydroxylases and Are Important for Nodulation[1][W][OA]

Juan Zhang, Senthil Subramanian, Yansheng Zhang[2], and Oliver Yu*

Donald Danforth Plant Science Center, St. Louis, Missouri 63132

Flavones are important copigments found in the flowers of many higher plants and play a variety of roles in plant adaptation to stress. In *Medicago* species, flavones also act as signal molecules during symbiotic interaction with the diazotropic bacterium *Sinorhizobium meliloti*. They are the most potent *nod* gene inducers found in root exudates. However, flavone synthase II (FNS II), the key enzyme responsible for flavone biosynthesis, has not been characterized in *Medicago* species. We cloned two FNS II genes from *Medicago truncatula* using known FNS II sequences from other species and named them MtFNSII-1 and MtFNSII-2. Functional assays in yeast (*Saccharomyces cerevisiae*) suggested that the catalytic mechanisms of both cytochrome P450 monooxygenases were similar to the other known legume FNS II from licorice (*Glycyrrhiza echinata*). MtFNSII converted flavanones to 2-hydroxyflavanones instead of flavones whereas FNS II from the nonlegume *Gerbera hybrida*, converted flavanones to flavones directly. The two MtFNSII genes had distinct tissue-specific expression patterns. MtFNSII-1 was highly expressed in roots and seeds whereas MtFNSII-2 was highly expressed in flowers and siliques. In addition, MtFNSII-2 was inducible by *S. meliloti* and methyl jasmonate treatment, whereas MtFNSII-1 was not. Histochemical staining of transgenic hairy roots carrying the promoter-reporter constructs indicated that the MtFNSII-2 induction was tissue specific, mostly localized to vascular tissues and root hairs. RNA interference-mediated suppression of MtFNSII genes resulted in flavone depleted roots and led to significantly reduced nodulation when inoculated with *S. meliloti*. Our results provide genetic evidence supporting that flavones are important for nodulation in *M. truncatula*.

Flavones are a group of phenolic secondary metabolites found in many higher plants. They are members of the diverse class of compounds collectively termed flavonoids. Flavones function as copigments in flowers, as antioxidants to protect plants from UV damage, and as phytoalexins with antimicrobial potentials (Dixon, 1986; Schmelzer et al., 1988; Yu et al., 2006). Flavones also play a role as signal molecules during the establishment of symbiosis between legumes and nitrogen-fixing rhizobia. Legumes secrete various flavonoid compounds into the rhizosphere as signal molecules. Specific flavonoids are recognized by NodD receptors on the cell surface of compatible rhizobial bacteria. This recognition induces the expression of *nod* genes responsible for the biosynthesis of Nod factors, a group of chitooligosaccharides that serve as the rhizobial signal molecules. When recognized by the plant roots, the Nod factors induce a set of morphological changes in roots that culminate in the formation of nitrogen-fixing nodules (Dakora et al., 1993).

The types of flavonoid secreted by the legume and the ability of the rhizobia's NodD receptor to recognize it are critical in determining host specificity (Honma et al., 1990). Plants of the genus *Medicago* are commonly colonized by the symbiotic partner *Sinorhizobium meliloti* (Hirsch et al., 2001). It was reported that the flavone luteolin from seed extracts of *Medicago* can specifically induce *nod* gene expression in *S. meliloti* (Peters et al., 1986). Since then, more detailed analysis has revealed that luteolin, apigenin, 7,4'-dihydroxflavone, and 4,4'-dihydroxy 2'-methoxy-chalcone are the most potent inducers of *S. meliloti nod* genes (Kapulnik et al., 1987; Orgambide et al., 1994). Of these compounds, only the 5-deoxy flavones have been identified in *Medicago* roots so far (Phillips et al., 1993; Coronado et al., 1995). In root exudates of *Medicago*, 7,4'-dihydroxflavone has been shown to accumulate under nitrogen starved conditions and hence is thought to be the physiologically important *nod* gene inducer (Zuanazzi et al., 1998). Despite flavones playing many important roles in *Medicago*, the key enzyme for their biosynthesis has not yet been characterized in these species and the function of flavones has not been studied using a genetic approach.

Flavones are produced through a branch of the phenylpropanoid pathway in all higher plants. The
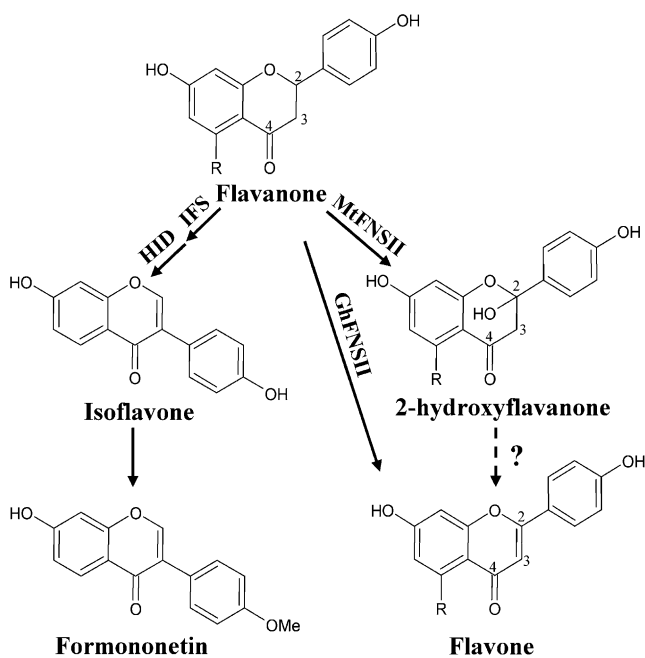
Figure 1. Partial diagram showing the flavone biosynthetic pathway. GhFNSII (CYP93B2) converts flavanones to flavones directly whereas MtFNSII produces a 2-hydroxyflavanone intermediate. The numbering schemes of carbon atoms are marked on the structures. The R group is either H or OH. When R = H (OH), the common names are liquiritigenin (naringenin), 2-hydroxyliquiritigenin (2-hydroxynaringenin), and 7,4′-dihydroxyflavone (apigenin), respectively. For isoflavones, only 5-deoxyisoflavonoids are shown.

key enzyme responsible for the biosynthesis of flavones is flavone synthase (FNS) and it converts flavanone substrates to flavones by introducing a double bond between C2 and C3 (Fig. 1). Enzymatic studies in *Petroselinium crispum* and *Antirrhinum majus* revealed the presence of two different enzyme systems for this reaction (Britsch et al., 1981). In *Petroselinium*, a soluble 2-oxoglutarate-dependent dioxygenase (FNS I) catalyzed this reaction; whereas an NADPH-dependent cytochrome P450 monooxygenase (FNS II) was responsible in *Antirrhinum*. Both enzymes can convert naringenin to apigenin and eriodoctyol to luteolin. FNS I has so far been identified only in members of the *Apiaceae* family (Martens et al., 2001); FNS II, however, is widespread (Martens and Mithofer, 2005).

Different catalytic mechanisms have been proposed for FNS I and FNS II. It was initially suspected that both enzymes add a hydroxyl group at the C2 first, followed by a dehydration reaction (Kochs et al., 1987). Interestingly, FNS II genes cloned from different species and expressed in heterologous systems showed two distinct types of activities. FNS II enzymes identified in species such as *Gerbera hybrida*, *A. majus*, and *Torrentia*, are thought to have a similar reaction mechanism as FNS I where the double bond is introduced by the abstraction of two vicinal hydrogen atoms in a radical-type mechanism. Heterologous expression of a licorice (*Glycyr-*

rhiza echinata) FNS II in yeast (*Saccharomyces cerevisiae*) and insect cells suggested that a 2-hydroxyflavanone intermediate is formed (Akashi et al., 1999), supporting the initial hypothesis. But no evidence exists for the enzymatic conversion of the intermediate into a flavone. In contrast, FNS II cloned from *G. hydrida* and other nonlegume species demonstrate a direct conversion to flavones without 2-hydroxyflavanone intermediates (Martens and Forkmann, 1999).

Here we report the cloning and functional characterization of two FNS II homologs from *M. truncatula*. We also provide genetic evidence for the important role of flavones in *Medicago* nodulation. Our results suggest that both MtFNSII enzymes have a catalytic mechanism similar to the other known legume FNS II from licorice. In addition, MtFNSII-1 (CYP90B10) and MtFNSII-2 (CYP90B11) have distinct tissue-specific expression patterns. Only MtFNSII-2 can be induced by *S. meliloti* and methyl jasmonate (MeJA) treatments, especially in the roots. RNAi-mediated suppression of MtFNSII led to significant reduction in nodule numbers, demonstrating that flavones are important for nodulation in *M. truncatula*.

RESULTS

Two Putative FNS II Genes Were Identified in the *M. truncatula* Genome

The Institute for Genomic Research (TIGR) *M. truncatula* EST database was BLAST searched using two known FNS II sequences from licorice GeFNSII (CYP93B1; Akashi et al., 1999) and *G. hybrida* GhFNSII (CYP93B2; Martens and Forkmann, 1999). Among the resulting matches with a complete open reading frame (ORF), a tentative contig (TC103414) with 79% homology to GeFNSII and 57% homology to GhFNSII was identified and chosen for further characterization. None of the other matching EST sequences had a significant homology to GeFNSII or GhFNSII. TC103414 had been annotated as a putative protein and included an ORF and a partial 3′ untranslated region. When the deduced amino acid sequence of TC103414 was compared to those of GeFNSII and GhFNSII, TC103414 appeared to be truncated at the N terminus, missing approximately 185 amino acids (data not shown), suggesting that it was an incomplete contig. MegaBLAST searches (Zhang et al., 2000) using this sequence against *M. truncatula* genomic sequence database (National Center for Biotechnology Information, http://www.ncbi.nlm.nih.gov/) resulted in the identification of the full-length genomic sequences of two putative FNSs that we designated as MtFNSII-1 (CYP93B10) and MtFNSII-2 (CYP93B11).

MtFNSII-1 and MtFNSII-2 had 98% identity at the amino acid level. The ORF regions between MtFNSII-1 and MtFNSII-2 shared 97% identity at the nucleic acid level. In contrast, the intron sequence structures were very divergent. MtFNSII-1 had one putative

617-bp-long intron as determined by sequence alignment against genomic sequence, while MtFNSII-2 had two introns of 70 and 591 bp length (Fig. 2).

Full-length cDNAs of MtFNSII-1 and MtFNSII-2 were cloned by reverse transcription (RT)-PCR from RNA of *M. truncatula* seedlings. Sequence analysis of MtFNSII-1 and MtFNSII-2 cDNAs revealed 77% and 78% identities, respectively, with GeFNSII. Both of them had 62% identities with GhFNSII. The deduced amino acid sequence of MtFNSII-1 shared 77% and 55% identity with GeFNSII and GhFNSII, respectively. MtFNSII-2 shared 78% identity with GeFNSII and 54% identity with GhFNSII. There were 11 amino acids different between the sequences of MtFNSII-1 and MtFNSII-2 coding regions. High identity at amino acid level between MtFNSII-1 and MtFNSII-2 suggested that both were most likely cytochrome P450s of *M. truncatula* that function as FNSs, while different intron pattern represented that they were different FNS II genes. The deduced amino acid sequences of MtFNSII genes were aligned to CYP93B1 (licorice, AB001380), CYP93B2 (*G. hybrida*, AF156976), CYP93B3 (*A. majus*, AB028151), CYP93B4 (*Torrentia hybrida*, AB028152), CYP93B5 (*Callistephus chinensis*, AF188612), CYP93B6 (*Perilla frutescens* var. *crispa*, AB045592), CYP93B9v1 (*Verbena x hybrida*, AB234903), CYP93B12 (*M. truncatula*, DQ335809), and CYP93B13 (*Gentiana triflora*, AB193314). Of the sequences compared, MtFNSII-1 and MtFNSII-2 were most homologous to GeFNSII (Fig. 3). The comparison among CYP93B1, MtFNSII-1 (CYP93B10), and MtFNSII-2 (CYP93B11) showed that both of them had the conserved function motifs of P450 (data not shown).

In Vivo Yeast Expression Assays Showed That MtFNSII-1 and MtFNSII-2 Are Functional FNSs

Functional assays of FNS II activity were performed by testing the ability of yeast cells expressing MtFNSII to convert flavanones into flavones. Vectors pESC-HIS-MtFNSII-1, pESC-HIS-MtFNSII-2, pYES2-GhFNSII (see "Materials and Methods") as a positive control, and the pESC-HIS and pYES2 vectors as negative controls, were transformed into WAT11 yeast cells independently. The WAT11 strain contains an Arabidopsis (*Arabidopsis thaliana*) cytochrome P450:NADPH reductase (Urban et al., 1997), which provides the reducing equivalents essential for the activity of plant cytochrome P450s such as FNS II.

Yeast cells expressing GhFNSII were able to metabolize naringenin to apigenin as well as liquiritigenin, a legume-specific flavanone to 7,4′-dihydroxyflavone as previously reported by Martens and Forkmann (1999). The cells expressing MtFNSII-1 and MtFNSII-2 also converted naringenin to apigenin (Fig. 4) and liquiritigenin to 7,4′-dihydroxyflavone (Supplemental Fig. S1), respectively. The control yeast cells carrying the empty vectors did not produce any apigenin (Fig. 4) or 7,4′-dihydroxyflavone (Supplemental Fig. S1). The identities of apigenin and 7,4′-dihydroxyflavone pro-

duced by the expressing yeast cells of MtFNSII-1, MtFNSII-2, and GhFNSII, respectively, were confirmed by comparison of UV absorption spectra and by liquid chromatography (LC)-mass spectrometry (MS) analysis (data not shown). This suggested that both MtFNSII-1 and MtFNSII-2 are indeed functional FNSs.

MtFNSII-1 and MtFNSII-2 Converted Flavanone Substrates to 2-Hydroxyflavanones

While yeast cells expressing MtFNSII-1, MtFNSII-2, or GhFNSII showed the production of apigenin from naringenin, an unknown peak was observed in addition to apigenin in extracts from yeast cells expressing MtFNSII-1 and MtFNSII-2 (Fig. 4), but not those expressing GhFNSII. Similarly, when fed with liquiritigenin, yeast cells expressing MtFNSII-1 and MtFNSII-2 produced an unknown peak partially overlapping with 7,4′-dihydroxyflavone, which was not seen in extracts from cells expressing GhFNSII (Supplemental Fig. S1). These unknown peaks had UV-absorption spectra similar to their respective substrates, naringenin (Fig. 5, A and B) and liquiritigenin (data not shown). The peaks were isolated by fractionation from HPLC and subjected to LC-MS analysis. The narigenin derived product had a molecular ion with a mass-to-charge ratio (m/z^+) of 289, compared to naringenin's molecular ion of m/z^+ 273 (Fig. 5, C and D), indicating that the unknown product could be a hydroxyl derivative of naringenin. We hypothesized that the unknown product was 2-hydroxy-naringenin, the catalytic product of GeFNSII (CPY93B1) using naringenin as
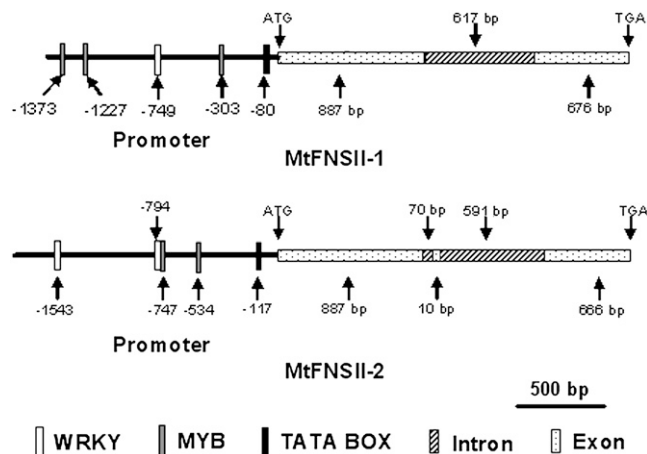

Figure 2. Structural diagram of MtFNSII-1 and MtFNSII-2 genes. The top drawing shows promoter and gene structure of MtFNSII-1. An 887-bp exon and a 676-bp exon are separated by one 617-bp intron. The bottom part shows the structure of MtFNSII-2 promoter and gene. Exons 1 to 3 are split by two introns. The length of the gene is in base pairs as shown in the size bar. The locations of various putative cis-elements of interests in promoter sequence, as identified using the PLACE database signal scan search (Higo et al., 1999), have been indicated. White box with dots represents exon; white box with dark upward diagonal lines is intron; white box is WRKY transcription factor binding motif; gray box is MYB transcription factor binding motifs; and black box is TATA box.
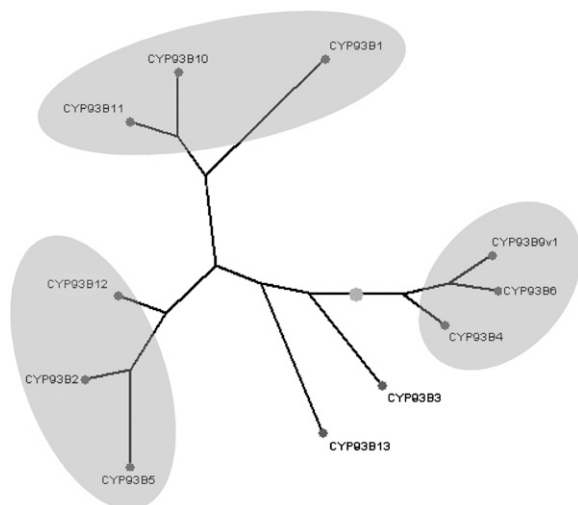
Figure 3. Phylogenetic comparison of deduced amino acid sequences of select FNS II-like genes from higher plants and green algae. FNS IIs were grouped into families based on sequence homology and substrate specificity. The FNS II sequences and corresponding GenBank accession numbers represented in this figure are as follows: CYP93B1 (licorice, AB001380), CYP93B2 (*G. hybrida*, AF156976), CYP93B3 (*A. majus*, AB028151), CYP93B4 (*T. hybrida*, AB028152), CYP93B5 (*C. chinensis*, AF188612), CYP93B6 (*P. frutescens* var. *crispa*, AB045592), CYP93B9v1 (*V. hybrida*, AB234903), CYP93B12 (*M. truncatula*, DQ335809), and CYP93B13 (*G. triflora*, AB193314). Of the sequences identified, MtFNSII-1 (CYP93B10) and MtFNSII-2 (CYP93B11) were most homologous to GeFNSII (CYP93B1) with 77% and 78% identity, respectively. Shaded ovals signify subfamily groupings.

substrate (Akashi et al., 1998). The major MS fragmentation products of naringenin were m/z^+ 153 and 147, which could only be derived from fragmentation at sites a and b (Fig. 5E), as well as c and d, respectively (Fig. 5E). In contrast, the unknown peak showed predominant fragmented ions of m/z^+ 153 and 121. The m/z^+ 153 ion could be derived from fragmentation at either a and b or b and c of 2-hydroxy-naringenin (Fig. 5F). The m/z^+ 121 ion could be derived from fragmentation at either a and d, or a and e (Fig. 5F). This observation strongly suggested that the molecular structure of the unknown peak was that of 2-hydroxy-naringenin.

The mass spectrum of liquiritigenin-derived product showed an m/z^+ of 273 compared to liquiritigenin's molecular ion of m/z^+ 256. The major MS fragmentation products of liquiritigenin were of m/z^+ 137 and 119, which could only be derived from fragmentation at sites a and b (Supplemental Fig. S2A). In contrast, the product of unknown peak showed predominant molecular ion of m/z^+ 137 and 121. The m/z^+ 137 ion could be derived from fragmentation between a and b of a 2-hydroxy-liquiritigenin (Supplemental Fig. 2B) while the m/z^+ 121 ion could be derived from fragmentation at sites b and c (Supplemental Fig. S2B). This observation suggested that the molecular structure of the unknown product was that of 2-hydroxy-liquiritigenin. In fact, all the most abun-

dant MS fragment ions, four each from the unknown products derived from naringenin and liquiritigenin by MtFNSII-1 and MtFNSII-2 could be fit perfectly into 2-hydroxy-flavanone structures (Fig. 5; Supplemental Fig. S2; analysis not shown), leading to the conclusion that the unknown peaks are 2-hydroxyflavanones. This suggested that the reaction mechanisms of both *M. truncatula* FNSs were very similar to that of the other legume FNS II reported from GeFNSII (Akashi et al., 1999).

We attempted in vitro assays using microsome preparations from yeast cells expressing the recombinant MtFNSII-1. When these microsomes were incubated with naringenin and the NADPH cofactor, the production of 2-hydroxy-naringenin could be detected in just 1 h (Supplemental Fig. S3) and continued to increase upon longer incubation up to 4 h. However, apigenin could be hardly detected even after 8 h in our in vitro assays (Supplemental Fig. S3). Similar results were observed when liquiritigenin was used as the substrate (data not shown). Apigenin production was observed in in vivo yeast assays but not in in vitro assays using yeast microsomes. Again, this suggested that MtFNSIIs converted flavanones into 2-hydroxy-flavanones and an unknown yeast enzyme could be
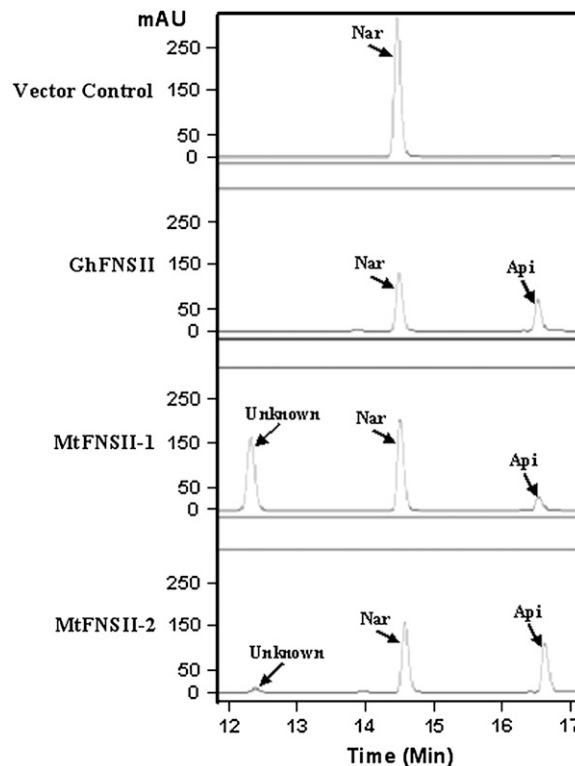

Figure 4. Reversed-phase HPLC profiles of extracts from yeast cells expressing GhFNSII, MtFNSII-1, or MtFNSII-2. Partial HPLC chromatograms show the production of apigenin (Api) from naringenin (Nar) by GhFNSII, MtFNSII-1, and MtFNSII-2. Yeast cells expressing MtFNSII-1 or MtFNSII-2 produce an unknown peak (Unknown; Rt = 12.35 min) not seen in GhFNSII reactions.

responsible for the conversion to the final product flavones in vivo.

MtFNSII-1 and MtFNSII-2 Have Distinct Tissue-Specific Expression Patterns

To investigate the biological functions of MtFNSII-1 and MtFNSII-2, gene expression patterns of both MtFNSII genes in various organs were analyzed by real-time quantitative (Q)RT-PCR. Total RNA was extracted from the roots, shoots, flowers, leaves, and siliques of *M. truncatula* and reverse transcribed to cDNAs. Transcript levels of both genes in these preparations were normalized against those of a ubiquitin gene (TC100151) in each tissue. MtFNSII-1 was highly expressed in roots (Fig. 6). This was consistent with the roles of flavones in microbial symbiosis in the roots. MtFNSII-1 was also expressed at relatively high levels in other tissues, which might be explained by their roles as UV protectant, defensive phytoalexin, and/or copigments in the flowers. The transcript levels of MtFNSII-2 were higher in flowers and siliques than in stems and leaves, while in roots MtFNSII-2 transcripts were hardly detectable (Fig. 6).

We further tested the effects of nodulation and defense signals on the expression of both *M. truncatula* FNS genes. Transcript levels of both genes were assayed in RNA preparations from *M. truncatula* seedlings treated with *S. meliloti* and MeJA. In response to those two different treatments, the transcript levels of MtFNSII-1 were not significantly altered (Supplemental Fig. S4), while MtFNSII-2 was obviously induced by *S. meliloti* (Supplemental Fig. S4) and MeJA, re-

spectively (data not shown). It suggested that the normal levels of root flavones could be increased by induced expression of MtFNSII-2, in addition to the constant levels of MtFNSII-1.

The Promoters from the Two MtFNSII Genes Have Different Expression Patterns in Transgenic Hairy Roots

Since flavones have been suggested to be important signal molecules during *M. truncatula-Sinorhizobium* interactions, the expression pattern of both MtFNSIIs in the roots were examined in more detail. The 5′ upstream elements of the MtFNSII-1 (approximately 1.5 kb) and MtFNSII-2 (approximately 1.9 kb) genes were cloned by PCR based on *M. truncatula* genomic sequences obtained from genome sequencing projects. The putative cis-elements of interest were identified using the PLACE software (Higo et al., 1999; http://www.dna.affrc.go.jp/htdocs/PLACE/) and indicated in Figure 2. Both promoters contained a putative TATA box (−80 bp in MtFNSII-1 and −117 bp in MtFNSII-2) upstream of the start codon, and putative binding motifs of MYB and WRKY transcription factors (Fig. 2).

A bacterial *uidA* (GUS) reporter cassette was placed under the control of these MtFNSII promoters and their tissue-specific expression patterns were examined in transgenic hairy roots composite plants by histochemical staining. GUS staining of 21-d-old roots showed that the MtFNSII-1 promoter was active throughout the length of the root. In cross sections of the root, the highest GUS accumulation was seen in the vascular tissues (Fig. 7A) and obvious root hair expression was also detected, which was consistent with
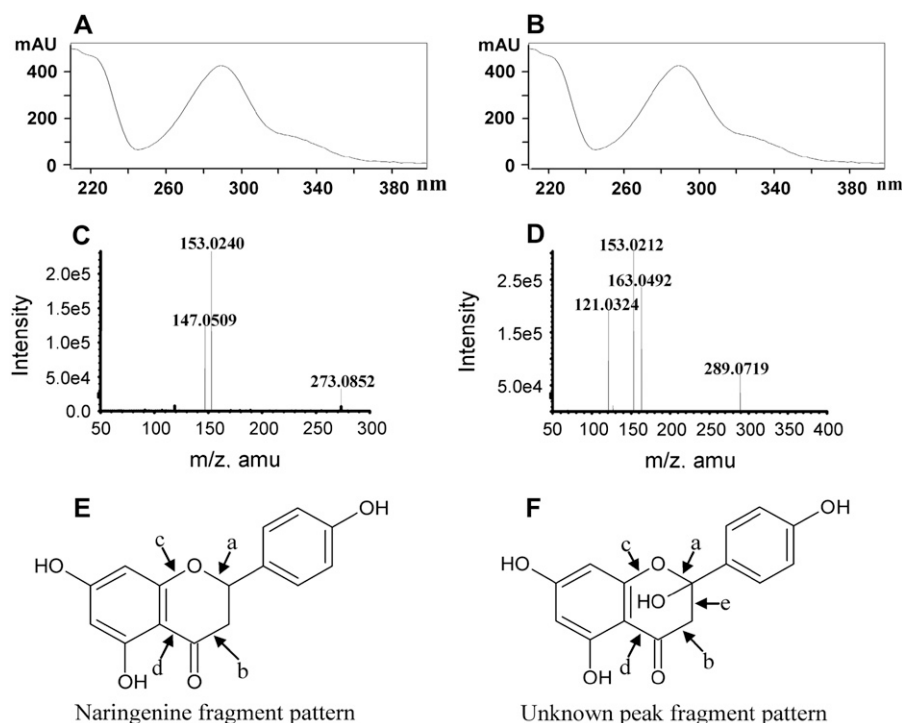

Figure 5. LC-MS analysis confirms the identity of unknown peak produced from narigenin as 2-hydroxynaringenin. UV-absorption spectra of naringenin (A) and the unknown peak (B) produced by MtFNSII are very similar. Upon LC-MS analysis, naringenin produced a molecular ion of m/z^+ 273 and product ions m/z^+ 153 and m/z^+ 147 (C), whereas the unknown product produced a molecular ion of m/z^+ 289 and product ions of m/z^+ 153, m/z^+ 121, and m/z^+ 163. Proposed sites of fragmentation indicated on the structure diagrams of naringenin (E) and the unknown product (F) indicate that the unknown product is 2-hydroxynaringenin.
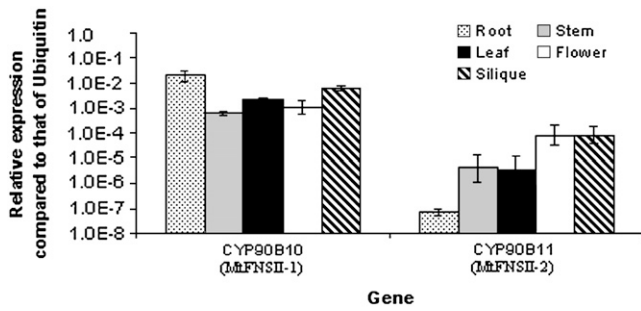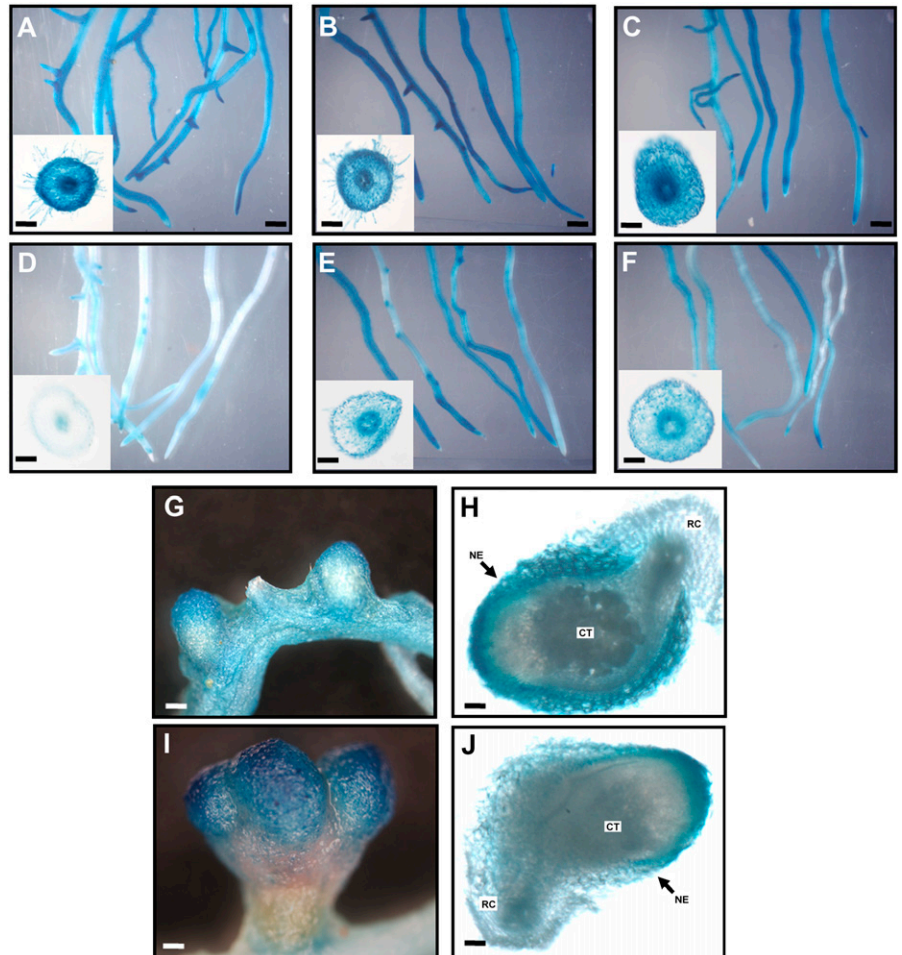
Naringenine fragment pattern

Unknown peak fragment pattern

Figure 6. Real-time RT-PCR analyses of MtFNSII-1 (CYP93B10) and MtFNSII-2 (CYP93B11) expression in different tissues of *M. truncatula*. Transcript levels were estimated using the relative C_t value method and normalized to that of *M. truncatula* Ubi gene. Error bars indicate the range of possible value based on SD of replicate C_t values. Data presented are representative of at least two independent experiments.

the presence of flavones in root exudates. While in the transgenic hairy roots using transformation of MtFNSII-2 promoter-GUS, the GUS gene expression was very weak and hardly detectable (Fig. 7D), which was consistent with the QRT-PCR results as shown above.

The transgenic composite plants were treated with *S. meliloti* for 6 h and MeJA for 8 h and the effect on MtFNSII-1 promoter-GUS and MtFNSII-2 promoter-GUS expression was examined. The expression pattern of MtFNSII-1 promoter-GUS expression pattern was not significantly altered among control and different treatments. In cross sections of the root, there was no obvious difference in the expression of MtFNSII-1 promoter-GUS among control, 8 h postinoculation with *S. meliloti*, or 6 h postinoculation with 100 μM MeJA (Fig. 7, A–C). However, treatments with MeJA and *S. meliloti* elevated the expression of MtFNSII-2 promoter-GUS. An obvious increase in GUS activities in almost all cell types was observed in the cross sections of the root (Fig. 7, D–F). The increase in MtFNSII-2 promoter-GUS activity in different sections correlated with increased transcript levels as shown by previous RT-PCR data.

We also stained the nodules on the transgenic roots transformed with MtFNSII-1 promoter-GUS and MtFNSII-2 promoter-GUS. GUS activity was observed in nodules of both transgenic hairy roots. With stronger expression in the MtFNSII-2 promoter-GUS lines than that of MtFNSII-1 lines (Fig. 7, G and H versus I and J). Once again, MtFNSII-2 was more significantly induced by *S. meliloti* than MtFNSII-1.

Figure 7. Tissue-specific distribution of MtFNSII-1 promoter-GUS and MtFNSII-2 promoter-GUS activities in transgenic hairy roots. MtFNSII-1 promoter is activated throughout the roots (A), while MtFNSII-2 promoter-GUS gene expression is very weak and hardly detected (D). The superficial GUS expression pattern of MtFNSII-1 promoter is not significantly altered with 8 h postinoculation with *S. meliloti* (B) and 6 h postinoculation with 100 μM MeJA (C). However, treatments with *S. meliloti* for 8 h (E) and MeJA for 6 h (F) induce a significant increase in expression of MtFNSII-2 promoter-GUS. Representative cross section of a transgenic hairy root at the corner showing GUS activity suggests that the increase in MtFNSII-2 promoter-GUS activity in the different sections seems to be due to a total increase in transcript levels. GUS activities are observed in the nodules on the transgenic hairy roots with transformation of MtFNSII-1 promoter-GUS (G and H) and MtFNSII-2 promoter-GUS (I and J). Scale bars in whole roots are 1 mm; in cross section of the roots are 100 μm; in G and I are 200 μm; H and J are 150 μm. CT, Nodule central tissue; RC, root cortex; NE, nodule epidermis.

Silencing of MtFNSII Leads to Reduced Nodule Numbers

The apparent root hair expressions of MtFNSII-1 and MtFNSII-2 induction by *S. meliloti* in roots seemed to support the role of flavones as the signal molecules for symbiotic rhizobia. To obtain genetic evidence for the role of MtFNSII in nodulation, we took an RNAi approach to silence the MtFNSII-1 and MtFNSII-2 expressions simultaneously in hairy roots. A 401-bp coding region with 97% identity between the two genes was amplified and cloned into an RNAi binary vector containing a GFP selectable marker. The construct was transformed into *M. truncatula* by *A. rhizogenes* to obtain hairy root composite plants. These plants consisted of transgenic hairy roots and untransformed shoot.

We tested the ability of our RNAi construct to silence the expression of MtFNSII genes in the root. As expected, the MtFNSII RNAi transgenic roots showed a significant reduction in MtFNSII expression when assayed by QRT-PCR (Fig. 8A). MtFNSII-1 transcripts were reduced by at least 18-fold. The MtFNSII-2 was not expressed in the roots and the transcripts were barely detected after RNAi. The effects of FNS silencing on root flavonoid profiles were assayed by HPLC analysis. Our data showed that approximately 90% of FNS RNAi roots had significantly lower levels of dihydroxyflavone, the major root flavone in *M. truncatula* when compared to vector control roots (Fig. 8B). Some of these transgenic roots had undetectable levels of dihydroxyflavone, indicating the RNAi construct effectively silenced the MtFNSII genes. Formononetin, a major isoflavone in the roots of *M. truncatula* showed a slight reduction as well. We could not detect any significant amount of the other flavones apigenin or leuteolin even in the wild type (or nontransgenic) root extracts.

Composite plants were inoculated with *S. meliloti* and the extent of nodulation was analyzed. In MtFNSII RNAi roots, the average number of nodules per root was reduced by about 50% when compared with that of vector control transgenic hairy roots (Fig. 8C). There was also a significant difference in the nodulation pattern between RNAi and control roots. The percentage of roots with less than five nodules was about 50% in the vector control roots, whereas it was about 76% in the MtFNSII RNAi roots. There was no significant difference in nodule numbers between transgenic (vector controls) and nontransgenic roots (data not shown), suggesting that hairy roots can support nodulation equally well. This direct genetic evidence suggested that flavone biosynthesis is indeed important to the nodulation of *M. truncatula* by *S. meliloti*.

DISCUSSION

Flavones in plants have multiple functions (Martens and Mithofer, 2005). In flowers of many plant species,

flavones are important copigments that alter the color of anthocyanins. Flavones are also important UV protectants in the aerial parts of plant. During plant defense responses, some plants accumulate significant amount of flavones as reservoirs of phytoalexins (Grotewold et al., 1998). Since the discovery that luteolin can specifically induce *nod* gene expression in *S. meliloti*, flavones have been speculated to play a major role in legume-rhizobium interactions as well, especially for the *Medicago* genus. To better understand these multiple roles of flavones, we identified two MtFNSII genes, investigated the biochemical properties of the enzymes, and studied their functions using gene expression analysis and RNAi silencing.
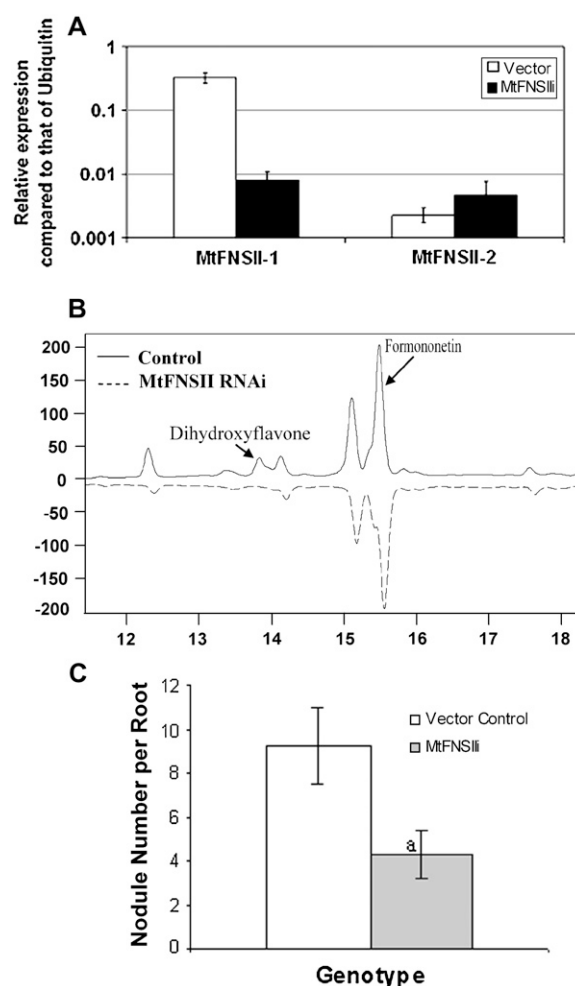

Figure 8. A, RNAi-mediated silencing of MtFNSII genes. Real-time RT-PCR analysis showed reduction of MtFNSII-1 gene and no significant changes in MtFNSII-2, which was not expressed in roots under normal conditions. B, RNAi-mediated MtFNSII silencing reduced dihydroxyflavone levels in *M. truncatula* hairy roots. C, Average nodule numbers per root in vector control (white bars); MtFNSII RNAi (gray bars) roots. Each data point is the average of at least 50 roots from 18 composite plants generated from three independent experiments. Error bars show SE of means. "a" indicates significant difference from the respective vector control, based on Poisson's distribution analysis ($P < 0.05$).

Two mechanisms of catalysis have been reported for FNS II enzymes. For example, FNS II from the legume licorice converts flavanones substrates to flavones via a 2-hydroxyflavanone intermediate, whereas FNS II from *G. hybrida* converts flavanones to flavones directly. Tests with different FNS enzymes showed that 2-hydroxynaringenin did not serve as a substrate for these enzymes and nor did it competitively inhibit the use of the flavanone substrate naringenin (Britsch, 1990). We discovered that the catalytic activities of both the FNS II enzymes from *M. truncatula* were similar to licorice FNS II in that they produced the intermediate, 2-hydroxyflavanone in yeast assays. It is not known why two different mechanisms exist. In licorice, 2-hydroxyflavanones are used as a substrate in the formation of the primary phytoalexin compound licodione (Akashi et al., 1999). Hence, it might have evolved to produce 2-hydroxyflavanones as an intermediate to be channeled to flavone or licodione biosynthesis. It is not known if *M. truncatula* produces any 2-hydroxyflavanones or their derivatives (other than flavones). However, there are several nonlegume plant species that produce 2-hydroxyflavanones derivatives (Grotewold et al., 1998), but biosynthetic enzymes from those species have not been characterized in detail. For example, maize (*Zea mays*) produces isovitexin, isoorientin, and isoscoparin, which are 2-hydroxyflavanone derivatives (Grotewold et al., 1998). In addition, species such as *Collinsonia candensis*, buckwheat (*Fagopyrum esculentum*), and *Mosla soochonensis* also produce 2-hydroxyflavanone derivatives. It will be interesting to characterize FNS II enzymes from these species to test their reaction mechanisms.

What is the possibility of the second mechanism being legume specific? Based on the deduced amino acid sequences of MtFNSIIs, only CYP93B1 (from licorice) was selected from TIGR Gene Indices using BLAST (Altschul et al., 1990). MtFNSIIs with CYP93B1 formed a distinct phylogeny branch with a much higher homology between each other, compared to nonlegume FNS II genes. They had a set of conserved amino acid that was not conserved in nonlegume FNS II enzymes. For example, Cys 98, Cys 276, and Cys 373 in legume FNS II genes corresponded to Ser, Val, and Ser, respectively, in nonlegume genes. These changes may eventually lead to different enzyme activity.

The expression patterns of the two MtFNSIIs were very different. Under normal conditions, MtFNSII-1 was expressed in all tissues, while MtFNSII-2 was predominantly expressed in the aerial part of the plants, especially in flowers. The expression pattern of these enzymes was consistent with the role of flavones in UV protection (in flowers) and symbiont chemoattraction (in roots). However, when *M. truncatula* seedlings were subjected to a defense signal (MeJA treatment) or a symbiotic signal (*S. meliloti* treatment), the normally quiescent MtFNSII-2 was highly induced in the roots. Both QRT-PCR assays and promoter-report expression studies suggested that the plants activated the MtFNSII-2 gene that was normally expressed in

other tissues, rather than boosting the constitutively root-expressed MtFNSII-1. One possible reason for this choice could be the coordinate activation of biosynthetic pathway enzymes upon defense (nodulation) signals (Ralston et al., 2005). Enzymes that form a complex together are coordinately regulated to enable proper channeling of metabolites. This is based on the putative metabolon model that is proposed to describe the organization of flavonoid enzymes (Winkel, 2004; Dixon, 2005; Ralston and Yu, 2006).

The tissue-specific expression pattern of MtFNSII-1 in the root hairs and vasculature was quite similar to what we observed for isoflavone synthase in soybean (*Glycine max*; Subramanian et al., 2004). Isoflavone synthase activity and isoflavone accumulation have been shown to be essential for nodulation in soybean (Subramanian et al., 2006). To obtain genetic evidence for the role of flavones in nodulation, an RNAi construct targeting both MtFNSII-1 and MtFNSII-2 was introduced into *M. truncatula* by establishing hairy root composite plants. The silencing was efficient, resulting in significantly reduced flavone levels in these roots. When inoculated with *S. meliloti*, there was a significant reduction in the number of nodules, suggesting that flavones are indeed important for the nodulation process. Recently it was shown in *M. truncatula* that silencing of chalcone synthase reduces nodulation and also affects auxin transport (Wasson et al., 2006). Chalcone synthase silencing, however, depletes the root of all flavonoids and hence it is not known which group of flavonoids are critical. We showed specifically that flavones play a major role in nodulation of *M. truncatula*. Interestingly, while regulation of auxin transport by flavonoids seems to be critical for nodulation in *M. truncatula* (Wasson et al., 2006), it is not critical in soybean (Subramanian et al., 2006). The role of isoflavones as endogenous *nod* gene inducers seems to be essential for nodulation in soybean. Further investigation is necessary to understand what role flavones play during nodulation in *M. truncatula* that is outside the scope of this report. Nevertheless, our results suggest that flavones are important during nodulation of *M. truncatula*.

MATERIALS AND METHODS

EST Sequence Analysis and Cloning of MtFNSII-1 and MtFNSII-2 cDNAs

Medicago truncatula EST sequences homologous to GeFNSII from licorice (*Glycyrrhiza echinata*; CYP93B1; Akashi et al., 1998) and GhFNSII from *Gerbera hybrida* (CYP93B2; Martens and Forkmann, 1999) were selected from TIGR Gene Indices (http://www.tigr.org/tigr-scripts/tgi/T_index.cgi?species=medicago) using a BLAST search (Altschul et al., 1990). One sequence was selected (TC103414) as a putative partial FNS II cDNA. MegaBLAST searches (Zhang et al., 2000) using this sequence against *M. truncatula* genomic sequence database (National Center for Biotechnology Information, http://www.ncbi.nlm.nih.gov/) resulted in the identification of the full-length genomic sequence of two putative FNSs named as MtFNSII-1 (CYP93B10) and MtFNSII-2 (CYP93B11), respectively. To obtain the full-length cDNA (MtFNSII), RT-PCR primers were designed based on the bacterial artificial chromosome sequences (Supplemental Table S1). The corresponding cDNAs

were cloned by RT-PCR using total RNA preparations from *M. truncatula* 'Jemalong A17' seedlings obtained by Trizol (Invitrogen). RT-PCR products were cloned into pGEM-T-easy vector (Promega) and then resequenced. Sequence alignments were performed using the AlignX module of Vector NTI (Invitrogen).

In Vivo Functional Analysis of Both MtFNSII-1 and MtFNSII-2 in Yeast

The coding regions of MtFNSII-1 and MtFNSII-2, starting from the ATG start codon and ending at the stop codon, were cloned into the pESC-HIS yeast (*Saccharomyces cerevisiae*) expression vector (Stratagene) under the control of a *Gal10* promoter at the multicloning sites. The primers used for cloning are showed in Supplemental Table S1. GhFNSII (CYP93B2) was previously cloned into the pYES2 yeast expression vector and was kindly provided by Dr. Stefan Martens (Martens and Forkmann, 1999). The above constructs, as well as the pESC-HIS and pYES2 vector as controls, were transformed into WAT11 cells (Pompon et al., 1996; Urban et al., 1997) made competent with the Frozen-EZ Yeast Transformation II kit (Zymo Research).

In vivo yeast assays were carried out as previously described with minor modifications (Ralston et al., 2005). Yeast cultures (2 mL) were grown overnight at 30°C in appropriate SD dropout liquid media (CLONTECH) containing 2% (w/v) Glc. Then cultures were collected by centrifugation and washed three times in sterile deionized water. Cultures were then resuspended to an OD_{600} of 1.0 in induction medium, i.e. SD dropout containing 2% (w/v) Gal. The substrate naringenin or liquiritigenin was then added to a final concentration of 50 to 100 μM. Approximately 12 to 16 h after induction, aliquots of cultures (400 μL) were extracted with equal volume of ethyl acetate. Extracts were concentrated to dryness with an Eppendorf Vacufuge (Eppendorf Scientific) at 45°C and redissolved in 80% methanol for subsequent HPLC analysis.

HPLC and LC-MS Analysis

Aliquots of the above extracts were analyzed on an Agilent 1100 series HPLC system using a Spherisorb ODS-2 reverse-phase C-18 column (5 μm; 250 × 4.6 mm) following previous methods (Akashi et al., 1999; Ralston et al., 2005). Samples were diluted into methanol and then separated using an 18-min linear gradient from 20% methanol:80% 10 mM ammonium acetate, pH 5.6, to 100% methanol at a flow rate of 1 mL min^{-1}. Elution of metabolites was monitored by a photodiode array. Retention time and UV spectra were compared to those of authentic standards when available.

For LC-MS analysis, fractions containing the targeted peaks were manually collected, dried under nitrogen, and dissolved in methanol containing 0.1% formic acid. An Applied Biosystems QSTAR XL hybrid quadrupole time-of-flight MS system equipped with a nanoelectrospray source (Protana XYZ manipulator) was used to confirm the identities of various metabolites. The nanoelectrospray was generated from a PicoTip needle (New Objectives) at 1,500 V. The two declustering potential parameters and focusing potential, i.e. DP, DP2, and FP, were 120, 10, and 230 V, respectively. Authentic standards were obtained from Indofine Chemical Company.

In Vitro MtFNSII Enzyme Activity Assay

Microsomes of yeast strain WAT11 expressing MtFNSII were prepared as described previously (Pompon et al., 1996). The protein content of each microsome preparation was assayed using the Bradford protein microassay (Bio-Rad). The in vitro microsomal enzyme assay was carried out as previously described (Yu et al., 2000). Briefly, approximately 80 μg of microsomal proteins were incubated at 30°C in a reaction buffer containing 80 mM K_2HPO_4 (pH 8.0), 0.5 mM glutathione, with 100 μM naringenin as the substrate and 0.4 mM NADPH as the cofactor. The reactions were stopped after the required time of incubation and extracted with ethyl acetate and analyzed by HPLC and LC-MS as described above.

Real-Time RT-PCR Analysis of MtFNSII-1 and MtFNSII-2 Expression

Total RNA was isolated from roots, stems, leaves, flowers, and immature siliques of *M. truncatula* using Trizol (Invitrogen) and treated with DNase I

to remove contaminating genomic DNA. First-strand cDNA was reverse transcribed using Moloney murine leukemia virus reverse transcriptase (New England Biolabs). QRT-PCR was performed with SYBR-Green using an iCycler thermocycler (Bio-Rad; Subramanian et al., 2005). Estimates of initial transcript concentrations were performed using the comparative threshold cycle method (Bovy et al., 2002; Subramanian et al., 2004). Transcript abundance of *M. truncatula* Ubiquitin gene (TC100151) in each RNA preparation was used as an internal standard. For MeJA treatment, 10-d-old seedlings (1–2 cm in length) of *M. truncatula* grown on filter papers were sprayed with a final concentration of 100 μM MeJA in nitrogen-free nutrient solution. Root and shoot tissues were collected after 6 h treatment. *Sinorhizobium meliloti* 1021 culture condition was described as previously (Subramanian et al., 2005). *M. truncatula* seedlings were flood inoculated by applying 5 mL of the rhizobia suspension to the root system. After 8 h, the root and shoot tissues were collected. The seedlings without any treatment were used as the hour 0 controls. Total RNA was isolated and treated with DNaseI. Transcript levels were analyzed using real-time RT-PCR as described above. The primers for real-time RT-PCR were showed in Supplemental Table S1.

Construction of Plant Transformation Vectors

The RNAi vector used to silence MtFNSII transcripts was constructed as previously described for isoflavone synthase RNAi (Subramanian et al., 2005). A 401-bp coding region that was more than 99% identical between MtFNSII-1 and MtFNSII-2 was amplified by PCR using primers that contained two sets of restriction sites (Supplemental Table S1). The PCR products were cloned into the CGT2255 shuttle vector (a kind gift from Dr. Chris Taylor, Donald Danforth Plant Science Center) in opposite orientations on either side of a pKANNIBAL intron to create an invert repeat driven by the figwort mosaic virus promoter (Subramanian et al., 2005). This MtFNSII RNAi construct was then cloned into pCAM-sUbi:GFP that was obtained by removing the 35S:GUS fragment from pCAMGFPGUS (Subramanian et al., 2004). The newly constructed pCAMGFP-MtFNSII-RNAi vector was transformed into *Agrobacterium rhizogenes* K599 by electroporation.

The promoters of MtFNSII-1 and MtFNSII-2 were PCR amplified, based on the sequence information from genomic bacterial artificial chromosome clone AC146789. A 1,489-bp fragment upstream of the MtFNSII-1 coding region and a 1,825-bp fragment upstream of MtFNSII-2 coding region were isolated. The PCR products were digested and inserted into a modified Gateway entry vector pMH40-ENTR4 (Invitrogen). The promoters were introduced into a pHGWFS7 Gateway expression vector (Karimi et al., 2002) by RL recombinase (Invitrogen). In these two pHGWFS7-MtFNSII-promoter-GUS vectors, the *uidA* gene was driven by the MtFNSII-1 and MtFNSII-2 promoter, respectively.

Generation of Composite Plants and Histochemical Analysis of GUS Expression

Seedlings of *M. truncatula* were grown in greenhouse for a month and used for transformation.

The hairy root composite plants were generated using the pCAMGFP-MtFNSII-RNAi vector or the pHGWFS7-MtFNSII-promoter-GUS vectors, following previously described methods (Subramanian et al., 2004; Collier et al., 2005). After 3 weeks, the transgenic composite plants were transferred to sand in the greenhouse. One week later, the plants were flood inoculated with *S. meliloti* as follows. Growth conditions for *S. meliloti* strain rm1021 (a kind gift from Dr. Terry Graham, Ohio State University, Columbus, OH) were the same as for *Bradyrhizobium japonicum* as described previously (Subramanian et al., 2004). *S. meliloti* cells were harvested by centrifugation and resuspended to an OD_{600} of 0.08 using nitrogen-free plant nutrient solution (McClure and Israel, 1979). Transgenic composite plants in sand were flood inoculated by applying 5 mL of the above bacterial suspension to the root system. Two weeks later, the roots were tested for GFP epifluorescence to identify transgenic roots. Nodules were then counted on each root. Nodule counts were analyzed for randomness in time and space using Poisson distribution and χ^2 statistical analyses (http://helios.bto.ed.ac.uk/bto/statistics/tress1.htm). For flavonoid analysis in roots, 100 mg transgenic roots were powdered by grinding under liquid N_2 and extracted with 500 μL 80% methanol. The supernatant was treated at 98°C for 2 h using 3 volumes of 1 N HCl, extracted with ethyl acetate and analyzed by HPLC as above.

Transgenic roots carrying the pHGWFS7-MtFNSII-promoter-GUS vectors were treated using MeJA for 6 h, *S. meliloti* for 8 h, or short wavelength UV for 2 h, respectively. Transgenic hairy roots, without the treatment as the 0 h controls and with different treatments were selected by GFP epifluorescence and then immersed in a GUS-staining solution [0.05% 5-bromo-4-chloro-indolyl-β-D-glucuronide in 100 mM sodium phosphate buffer, pH 7.0, containing 10 mM EDTA, 0.1% Triton, and 0.5 mM K$_4$Fe(CN)$_6$ 6H2O] and allowed to stain for 16 h at room temperature (Jefferson et al., 1987). To stop GUS staining, the roots were removed from the staining solution and washed with 70% ethanol. The GUS staining pattern was visualized with a dissecting microscope (Olympus SZX12). The transgenic hairy roots with nodules were also stained using the GUS staining solution.

Supplemental Data

The following materials are available in the online version of this article.

Supplemental Figure S1. Reversed-phase HPLC profiles of extracts from yeast cells expressing GhFNSII, MtFNSII-1, or MtFNSII-2.

Supplemental Figure S2. LC-MS analysis confirms the identity of unknown peak produced from liquiritigenin as 2-hydroxyliquiritigenin.

Supplemental Figure S3. MtFNSII-1 or MtFNSII-2 converts flavanones into 2-hydroxyflavanones and not flavones.

Supplemental Figure S4. Real-time RT-PCR analyses of MtFNSII-1 (CYP93B10) and MtFNSII-2 (CYP93B11) expression in treatment with *S. meliloti*.

Supplemental Table S1. PCR primers used in this study.

Note Added in Proof

The authors would like to bring to the readers' attention the possibility that the product of MtFNSII putatively identified as 2-hydroxyliquiritigenin (Supplemental Fig. S2) could be licodione [1-(2,4-dihydroxyphenyl)-3-(4-hydroxyphenyl)-1,3-propanedione] that exists in a tautomeric mixture of diketonic and ketoenolic forms. 2-Hydroxyliquiritigenin is another theoretical tautomer of licodione, but this hemiacetal form is unstable and can be spontaneously converted into open-chain forms (**Ayabe S, Kobayashi M, Hikichi M, Matsumoto K, Furuya T** [1980] Flavonoids from the cultured cells of *Glycyrrhiza echinata*. Phytochemistry **19:** 2179–2183; **Ayabe S, Furuya T** [1980] ^{13}C NMR studies on licodione and related compounds in equilibrium mixture of keto and enol forms. Tetrahedron Lett **21:** 2965–2968).

ACKNOWLEDGMENTS

LITERATURE CITED

Akashi T, Aoki T, Ayabe S (1998) Identification of a cytochrome P450 cDNA encoding (2S)-flavanone 2-hydroxylase of licorice (*Glycyrrhiza echinata* L.; Fabaceae) which represents licodione synthase and flavone synthase II. FEBS Lett **431:** 287–290

Akashi T, Aoki T, Ayabe S (1999) Cloning and functional expression of a cytochrome P450 cDNA encoding 2-hydroxyisoflavanone synthase involved in biosynthesis of the isoflavonoid skeleton in licorice. Plant Physiol **121:** 821–828

Altschul SF, Gish W, Miller W, Myers EW, Lipman DJ (1990) Basic local alignment search tool. J Mol Biol **215:** 403–410

Bovy A, de Vos R, Kemper M, Schijlen E, Pertejo MA, Muir S, Collins G, Robinson S, Verhoeyen M, Hughes S (2002) High-flavonol tomatoes

resulting from the heterologous expression of the maize transcription factor genes LC and C1. Plant Cell **14:** 2509–2526

Britsch L (1990) Purification and characterization of flavone synthase I, a 2-oxoglutarate-dependent desaturase. Arch Biochem Biophys **282:** 152–160

Britsch L, Heller W, Griesbach H (1981) Conversion of flananone to flavone, dihydroflavanol and flavonol with an enzyme system from cell cultures of parsley. Z Naturforsch **36c:** 742–750

Collier R, Fuchs B, Walter N, Kevin LW, Taylor CG (2005) Ex vitro composite plants: an inexpensive, rapid method for root biology. Plant J **43:** 449–457

Coronado C, Zuanazzi JAS, Sallaud C, Quirion JC, Esnault R, Husson HP, Kondorosi A, Ratet P (1995) Alfalfa root flavonoid production is nitrogen regulated. Plant Physiol **108:** 533–542

Dakora FD, Joseph CM, Phillips DA (1993) Alfalfa (*Medicago sativa* L.) root exudates contain isoflavonoids in the presence of *Rhizobium meliloti*. Plant Physiol **101:** 819–824

Dixon RA (1986) The phytoalexin response: eliciting, signalling and control of host gene expression. Biol Rev **61:** 239–291

Dixon RA (2005) Engineering of plant natural product pathways. Curr Opin Plant Biol **8:** 329–336

Grotewold E, Chamberlin M, Snook M, Siame B, Butler L, Swenson J, Maddock S, Clair GS, Bowen B (1998) Engineering secondary metabolism in maize cells by ectopic expression of transcription factors. Plant Cell **10:** 721–740

Higo K, Ugawa Y, Iwamoto M, Korenaga T (1999) Plant cis-acting regulatory DNA elements (PLACE) database. Nucleic Acids Res **27:** 297–300

Hirsch AM, Lum MR, Downie JA (2001) What makes the rhizobia-legume symbiosis so special? Plant Physiol **127:** 1484–1492

Honma MA, Asomaning M, Ausubel FM (1990) Rhizobium meliloti nodD genes mediate host-specific activation of nodABC. J Bacteriol **172:** 901–911

Jefferson RA, Kavanagh TA, Bevan MW (1987) GUS fusions—beta-glucuronidase as a sensitive and versatile gene fusion marker in higher-plants. EMBO J **6:** 3901–3907

Kapulnik Y, Joseph CM, Phillips DA (1987) Flavone limitations to root nodulation and symbiotic nitrogen fixation in alfalfa. Plant Physiol **84:** 1193–1196

Karimi M, Inze D, Depicker A (2002) GATEWAY vectors for Agrobacterium-mediated plant transformation. Trends Plant Sci **7:** 193–195

Kochs G, Welle R, Grisebach H (1987) Differential induction of enzyme in soybean cell cultures by elicitor or osmotic stress. Planta **171:** 519–524

Martens S, Forkmann G (1999) Cloning and expression of flavone synthase II from *Gerbera hybrids*. Plant J **20:** 611–618

Martens S, Forkmann G, Matern U, Lukacin R (2001) Cloning of parsley flavone synthase I. Phytochemistry **58:** 43–46

Martens S, Mithofer A (2005) Flavones and flavone synthases. Phytochemistry **66:** 2399–2407

McClure PR, Israel DW (1979) Transport of nitrogen in the xylem of soybean plants. Plant Physiol **64:** 411–416

Orgambide GG, Philip-Hollingsworth S, Hollingsworth RI, Dazzo FB (1994) Flavone-enhanced accumulation and symbiosis-related biological activity of a diglycosyl diacylglycerol membrane glycolipid from Rhizobium leguminosarum biovar trifolii. J Bacteriol **176:** 4338–4347

Peters NK, Frost JW, Long SR (1986) A plant flavone, luteolin, induces expression of Rhizobium meliloti nodulation genes. Science **233:** 977–980

Phillips DA, Dakora FD, Leon-Barrios M, Sande E, Joseph CM (1993) Signals released from alfalfa regulate microbial activities in the rhizosphere. Curr Plant Sci Biotechnol Agric **17:** 197–202

Pompon D, Louerat B, Bronine A, Urban P (1996) Yeast expression of animal and plant P450s in optimized redox environments. Methods Enzymol **272:** 51–64

Ralston L, Subramanian S, Matsuno M, Yu O (2005) Partial reconstruction of flavonoid and isoflavonoid biosynthesis in yeast using soybean type I and type II chalcone isomerases. Plant Physiol **137:** 1375–1388

Ralston L, Yu O (2006) Metabolons involving plant cytochrome P450s. Phytochem Rev **5:** 459–472

Schmelzer E, Jahnen W, Hahlbrock K (1988) In situ localization of light-induced chalcone synthase mRNA, chalcone synthase, and flavonoid endproducts in epidermal cells of parsley leaves. Proc Natl Acad Sci USA **85:** 2989–2993

Subramanian S, Graham MY, Yu O, Graham TL (2005) RNA interference of soybean isoflavone synthase genes leads to silencing in tissues distal to the transformation site and to enhanced susceptibility to *Phytophthora sojae*. Plant Physiol **137:** 1345–1353

Subramanian S, Stacey G, Yu O (2006) Endogenous isoflavones are essential for the establishment of symbiosis between soybean and Bradyrhizobium japonicum. Plant J **48:** 261–273

Subramanian S, Xu L, Lu G, Odell J, Yu O (2004) The promoters of the isoflavone synthase genes respond differentially to nodulation and defense signals in transgenic soybean roots. Plant Mol Biol **54:** 623–639

Urban P, Mignotte C, Kazmaier M, Delorme F, Pompon D (1997) Cloning, yeast expression, and characterization of the coupling of two distantly related Arabidopsis thaliana NADPH-cytochrome P450 reductases with P450 CYP73A5. J Biol Chem **272:** 19176–19186

Wasson AP, Pellerone FI, Mathesius U (2006) Silencing the flavonoid pathway in *Medicago truncatula* inhibits root nodule formation and prevents auxin transport regulation by rhizobia. Plant Cell **18:** 1617–1629

Winkel BSJ (2004) Metabolic channeling in plants. Annu Rev Plant Biol **55:** 85–107

Yu O, Jung W, Shi J, Croes RA, Fader GM, McGonigle B, Odell JT (2000) Production of the isoflavones genistein and daidzein in non-legume dicot and monocot tissues. Plant Physiol **124:** 781–794

Yu O, Matsuno M, Subramanian S (2006) Flavonoids in flowers: genetics and biochemistry. *In* JA Teixeira da Silva, ed, Floriculture, Ornamental and Plant Biotechnology: Advances and Topical Issues, Ed 1. Global Science Books, London, pp 283–293

Zhang Z, Schwartz S, Wagner L, Miller W (2000) A greedy algorithm for aligning DNA sequences. J Comput Biol **7:** 203–214

Zuanazzi JAS, Clergeot PH, Quirion JC, Husson HP, Kondorosi A, Ratet P (1998) Production of Sinorhizobium meliloti nod gene activator and repressor flavonoids from Medicago sativa roots. Mol Plant Microbe Interact **11:** 784–794